Journal of the Korean Physical Society, Vol. 57, No. 3, September 2010, pp. 563∼566

Excursion Set Statistics with Primordial Non-Gaussianity

Graziano Rossi,* Pravabati Chingangbam and Changbom Park
Korea Institute for Advanced Study, Seoul 130-722

(Received 17 December 2009)

The statistics of regions above and below a temperature threshold (excursion sets), fully characterized in the contest of Gaussian random fields, is here extended to models with primordial non-Gaussianity of the local type and is used to analyze the cosmic microwave background (CMB) sky via simulated non-Gaussian maps. In particular, a positive value of the non-Gaussian parameter $f_{\rm NL}$ is found to enhance the number density of the cold CMB excursion sets, along with their clustering strength, and to reduce that of the hot ones. This effect may be important to discriminate between the simpler Gaussian hypothesis and non-Gaussian scenarios, arising either from non-standard inflation or alternative early-universe models. However, while a distinct signature in the clustering of hot and cold pixels clearly emerges for large non-Gaussianity, particularly at angular scales of about 75 arcmin, the considered statistics appears to be less sensitive when $f_{\rm NL}$ is relatively small and an additional smoothing is applied. This fact may pose a challenge if using the excursion set regions to constrain $f_{\rm NL}$, or the Gaussianity itself, from a real data set – in presence of noise and other observational artifacts.

PACS numbers: 98.70.Vc, 98.80.Bp, 98.80.-k
Keywords: Statistical methods, Cosmic microwave background, Correlations, Cosmology, Observations.
DOI: 10.3938/jkps.57.563

I. INTRODUCTION

While there has been a recent revival on theoretical and observational studies of primordial non-Gaussianity [1–5], mainly because of the Wilkinson microwave anisotropy probe (WMAP) data which seems to favor a positive value of the non-Gaussian $f_{\rm NL}$ parameter [6], to date, the experimental detection of a significant deviation from the Gaussian paradigm remains far from convincing and still challenging. Gaussian random processes are theoretically desirable because they are the only ones for which the knowledge of all spectral parameters completely determines all the statistical properties; however, progress in inflation model building and in alternative early-universe scenarios has led to more complicated non-Gaussian statistical properties of fluctuations. These properties of the primordial perturbations are uniquely imprinted in the cosmic microwave background (CMB) anisotropy distribution; therefore, by analyzing the specifics of the primordial anisotropy we are effectively looking at the properties of the inflationary models (or alternatives to inflation) that describe the origin of the Universe. Deviations from Gaussian initial conditions have also important consequences for many aspects of the large-scale structure of the Universe, such as the statistics of voids or the distribution of neutral hydrogen, the topology, the reionization history and the abundance, clustering and biasing of dark matter halos [7–11].

If large-scale structure probes are important and complementary for studying non-Gaussianity, the CMB remains the cleanest and more direct tool to detect deviations from the Gaussian paradigm, although studies related to the microwave sky are complicated by a variety of experimental artifacts. This is essentially why a multitude of non-Gaussian estimators have been applied so far, and data from the WMAP mission has been used to constrain primordial non-Gaussianity with controversial results [4,6,12–14] and a long list of anomalies reported [15–17].

All these facts have motivates the quest for alternative statistics more sensitive to deviations from Gaussianity and the search for unique features that may represent a distinct signal of non-Gaussianity. To this end, in our previous work [18], we compared the pixel clustering statistics under Gaussian conditions against WMAP five-year data and detected some deviations from the theoretical expectations. In particular, we pointed out a remarkable difference in the clustering of hot and cold pixels at relatively small angular scales. Whether or not this difference may arise from a primordial non-Gaussianity of the local type is the main subject of this study. To achieve this goal, we focus on the intrinsic CMB by simulating non-Gaussian sky maps with different levels of $f_{\rm NL}$ and present a theoretical study about the feasibility

*E-mail: graziano@kias.re.kr

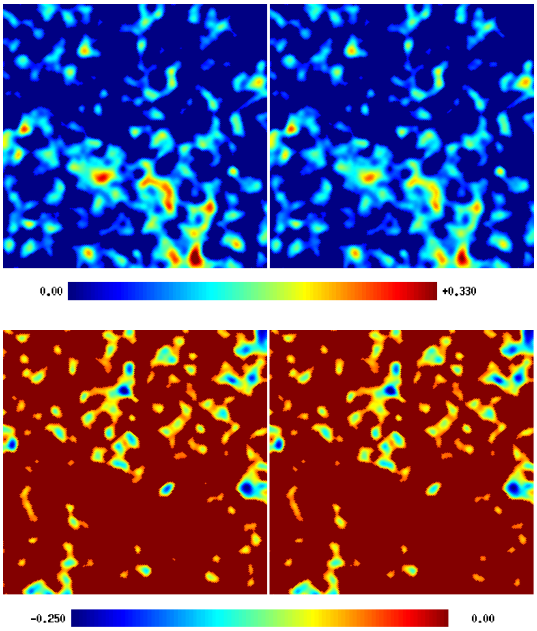

Fig. 1. (Color online) A small patch of the simulated CMB sky with primordial Gaussianity (left panels) and non-Gaussianity of the local type with $f_{\rm NL} = 500$ (right panels), smoothed with a Gaussian beam of FWHM $= 30'$. Regions below $\nu = 0.50$ (top panels) or above $\nu = -0.50$ (bottom panels) are set to zero. The temperature scale is in mK, ranging from 0 to +330 mK (top panels) or from 0 to -250 mK (bottom panels).

of using clustering statistics as a tool for constraining non-Gaussianity. While the ultimate goal is to compare our statistics against observations, and so to take into account all the possible sources of signal contamination like beam smearing, noise, foregrounds, point sources (subject of ongoing work), here we focus only on the intrinsic CMB as the first step in this process.

The layout of the paper is as follows: In Section II., we briefly describe the simulated maps used in this study. In Section III., we outline the the excursion set formalism and we present results for the number density and the clustering statistics of pixels averaged over 200 maps in the presence of non-Gaussianity of the $f_{\rm NL}$ type. Section IV. summarizes our findings and highlights ongoing work.

II. NON-GAUSSIAN SIMULATIONS

The simulated non-Gaussian maps adopted in this study are constructed following the method outlined in Ref. 19, and are described in detail in Ref. 20. Briefly, the CMB temperature fluctuations are expanded in terms of spherical harmonics as $\Delta T(\hat{n}) = \sum_{\ell m} a_{lm} Y_{lm}(\hat{n})$, and the $a_{\ell m}$'s are then computed by convolving the primordial potential fluctuations with the radiation transfer

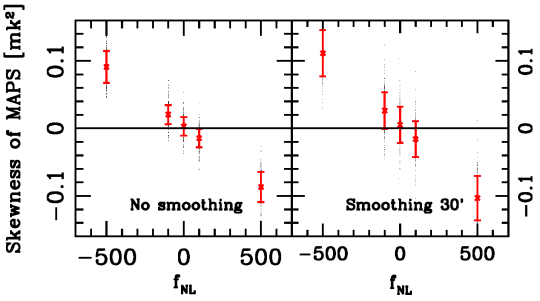

Fig. 2. Skewness of the simulated CMB maps as a function of $f_{\rm NL}$ averaged over 200 realizations, with no smoothing (left panel) or after application of a Gaussian beam with FWHM $= 30'$ (right panel). Differences are significant, even for a relatively low degree of non-Gaussianity.

function $\Delta_\ell(r)$, which can be determined independently using the well-known computer code CMBFAST [21]. In essence, the main point of the technique [19] is to calculate the $a_{\ell m}$'s as an integral in real, rather than Fourier, space. This is accomplished by properly rewriting the $a_{\ell m}$'s in a more suitable form, namely,

$$a_{\ell m} = \int {\rm d}r\, r^2 \Phi_{\ell m}(r) \Delta_\ell(r)\,, \qquad (1)$$

where $\Phi(\mathbf{k})$ is the Fourier transform of the real space potential $\Phi(\mathbf{r})$.

In the presence of non-Gaussianity of the $f_{\rm NL}$ type, one simply needs to modify the potential as $\Phi(\mathbf{k}) = \Phi^{\rm L}(\mathbf{k}) + f_{\rm NL}\Phi^{\rm NL}(\mathbf{k})$, where

$$\Phi^{\rm NL}(\mathbf{k}) = \int \frac{{\rm d}^3 k_1}{(2\pi)^3}\, \Phi^{\rm L}(\mathbf{k}+\mathbf{k_1})\, \Phi^{\rm L}(\mathbf{k_1}), \qquad (2)$$

and essentially repeat steps similar to those for the Gaussian case. The parameters adopted in the simulations are those from the WMAP 5-yr best fit, assuming a standard cold dark matter model (LCDM) with cosmological constant [6].

An example of these simulations is shown in Fig. 1 for a small patch of the sky, where regions below (upper panels) or above (bottom panels) a temperature threshold characterized by $|\nu| = \delta T/\sigma = 0.50$ are set to zero, with σ being the rms deviation of the temperature map and δT the temperature anisotropy. The left panels highlight the Gaussian case while the right panels show the corresponding non-Gaussian scenario with $f_{\rm NL} = 500$. A Gaussian smoothing with a full width at half maximum (FWHM) of 30 arcmin is applied to those regions. It is indeed very hard to notice any differences simply by visual inspection, even though the skewness of the two maps is quite different, as shown in Fig. 2 for the unsmoothed (left panel) and smoothed cases (right panel). Error bars represent the 1-σ deviations, estimated from 200 realizations.

III. STATISTICS OF EXCURSION SETS IN THE $F_{\rm NL}$ MODEL

1. Theoretical Formalism

In a full Gaussian sky and in the absence of pixel noise, the number density of regions above (below) a temperature threshold ν (excursion sets, see Fig. 1) is simply given by:

$$n_{\rm pix}(\nu) = N_{\rm pix,tot} \cdot {\rm erfc}(\nu/\sqrt{2})/8\pi, \quad (3)$$

where $N_{\rm pix,tot} = 12N_{\rm side}^2$ is the total number of pixels in the map at a resolution specified by the parameter $N_{\rm side}$. The corresponding clustering of patches above (below) ν is

$$1+\xi_\nu(\theta) = 2[{\rm erfc}(\nu/\sqrt{2})]^{-2}[\pi\sqrt{1-w^2(\theta)}]^{-1} \times \int_\nu^\infty {\rm d}\nu_1 \int_\nu^\infty e^{-\frac{\nu_1^2+\nu_2^2-2\nu_1\nu_2 w(\theta)}{2[1-w^2(\theta)]}} {\rm d}\nu_2, \quad (4)$$

where

$$w(\theta) = C(\theta)/\sigma = \sum_\ell \frac{(2\ell+1)}{4\pi} C_\ell^{\rm in} W_\ell^{smooth} P_\ell^0(\cos\theta)/\sigma; \quad (5)$$

$C_\ell^{\rm in}$ is the input power spectrum, and W_ℓ^{smooth} includes all the additional smoothing.

In presence of non-Gaussianity, the theoretical formalism is more complicated. Rather than attempting to derive it analytically, our approach here consists of using non-Gaussian simulations as the theory expectations, controlled by the well-known Gaussian case (Eqs. (3) - (5)). This is mainly because all observational artifacts are readily implemented in our pipeline whereas it would be problematic to include them within an analytic framework.

2. Analysis of Non-Gaussian Maps

Figure 3 shows the variation of the pixel number density above (below) the threshold with $f_{\rm NL}$, normalized by the expectation from Gaussian theory (Eq. 3). No smoothing is applied at a resolution $N_{\rm side} = 512$. Error bars are the 1-σ deviations estimated from 200 realizations. The low-threshold regions ($\nu = 0.25, 0.50$) or the area around $\nu = 2.00$ appear to be good candidates to distinguish a Gaussian case from a non-Gaussian one. The small fluctuations at higher thresholds are due to cosmic variance.

Figure 4 displays the difference (left panels) and the ratio (right panels) between the number density of the hot versus cold pixels at corresponding temperature thresholds when $f_{\rm NL} = 100$ (top panels) or $f_{\rm NL} = 500$ (bottom panels). Even in this case, the same two areas of interest mentioned before are clearly noticeable while the zone around $\nu = 1.00$ does not allow a Gaussian signal to be distinguished from a non-Gaussian one.

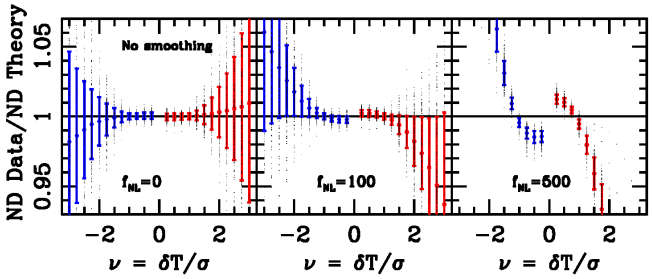

Fig. 3. (Color online) Number density of pixels above or below a temperature threshold normalized by the expectation from Gaussian theory (Eq. 3), for different values of $f_{\rm NL}$ as indicated in the panels. No smoothing is applied at $N_{\rm side} = 512$.

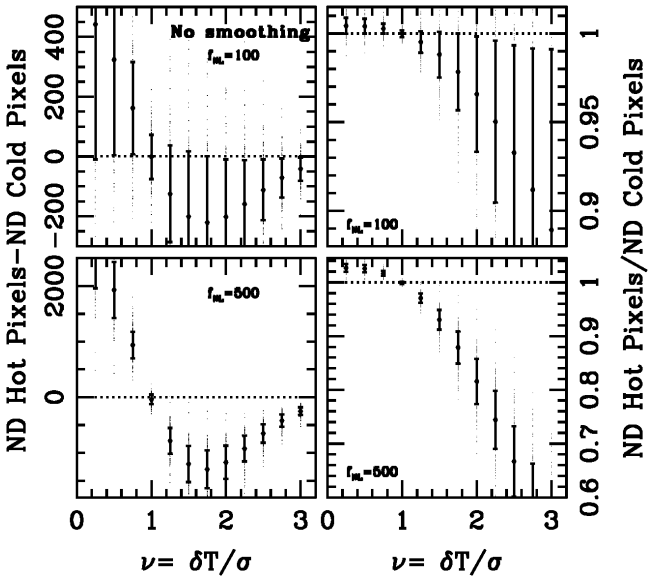

Fig. 4. Difference (left) and ratio (right) between the number density of hot and cold pixels at corresponding ν values, for different levels of non-Gaussianity, as indicated in the panels. Error bars are $1-\sigma$ estimates over 200 realizations.

An example of the clustering strength of pixels above $\nu = 2.00$ (one of the two interesting regions) is shown in Fig. 5 for the Gaussian case (left) or when $f_{\rm NL} = 500$ (right) with no smoothing. As expected, there is essentially no difference in clustering when the map is Gaussian whereas for a positive and large $f_{\rm NL}$, a significant enhancement of the cold pixels with respect to the hot ones appears (as for the number density in Fig. 3), particularly at angular scales around $\theta = 75'$. This effect is a distinct signature of non-Gaussianity of the local type; whether or not it may be useful in constraining $f_{\rm NL}$ from a real data set mainly depends on how to beat the effect of cosmic variance.

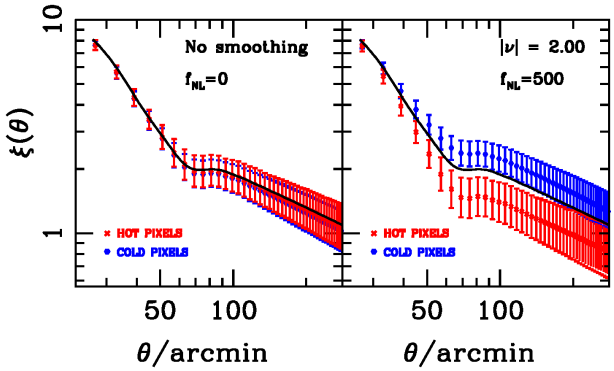

Fig. 5. (Color online) Clustering statistics of hot and cold CMB patches above (below) $|\nu| = 2.00$ for the Gaussian case (left) and in presence of local non-Gaussianity with $f_{\rm NL} = 500$ (right). Errors are $1-\sigma$ estimates over 200 realizations, and no smoothing is applied. The solid line in both panels is the theoretical expectation for the Gaussian case (Eq. 4).

IV. CONCLUSION

We presented the first step in applying the statistics of the CMB temperature excursion sets as a tool for constraining models with primordial local non-Gaussianity ($f_{\rm NL}$ type). This study was motivated by our previous findings, namely, a detection of a significant difference in the clustering of hot versus cold regions in the WMAP 5-yr data [18]. By using a set of simulated non-Gaussian maps (Figs. 1 and 2), the number density and the clustering of pixels above or below a temperature threshold were analyzed (Figs. 3 and 5), along with some other derived statistics (Fig. 4). When $f_{\rm NL} = 500$ a significant excess was confirmed, both in the number density and in the clustering of the cold versus hot pixels. Other important findings include the existence of two areas ($\nu = 0.25, 0.50$ and around $\nu = 2.00$) more sensitive to non-Gaussian effects, and an interesting scale of $\theta = 75'$ where deviations from Gaussianity are maximized.

While the effectiveness of this statistics in constraining non-Gaussianity from a real data set depends critically on how well one can beat cosmic variance, we are considering derived statistics that can maximize the non-Gaussian contribution. Including realistic effects, such as inhomogeneous noise, point source contamination or foregrounds, so that we can compare our simulated predictions with current observations is the subject of ongoing work.

ACKNOWLEDGMENTS

GR would like to thank Remo Ruffini, Sang Pyo Kim, Bum Hoon Lee, and the local organizing committee of the 11th Italian-Korean Symposium on Relativistic Astrophysics for the kind invitation. GR is also grateful to the Italian Embassy, and in particular to Ambassador Massimo Andrea Leggeri and Scientific Director Antonino Tata, for promoting and supporting scientific cooperation between Italy and Korea and to all the other sponsoring institutions (CQUeST, APCTP, ICRA, IEU, KASI, CNR, KOSEF) which made this meeting possible.

REFERENCES

[1] P. Creminelli, L. Senatore, M. Zaldarriaga and M. Tegmark, J. Cosmol. Astropart. Phys. **3**, 5 (2007).
[2] E. I. Buchbinder, J. Khoury and B. A. Ovrut, Phys. Rev. Lett. **100**, 171302 (2008).
[3] S. Matarrese and L. Verde, Astrophys. J. **677**, L77 (2008).
[4] D. N. Spergel *et al.*, Astrophys. J. **170**, 377 (2007).
[5] C. Hikage, T. Matsubara, P. Coles, M. Liguori, F. K. Hansen and S. Matarrese, Mon. Not. R. Astron. Soc. **389**, 1439 (2008).
[6] E. Komatsu *et al.*, Astrophys. J. S. **180**, 330 (2009).
[7] M. Lo Verde, A. Miller, S. Shandera and L. Verde, J. Cosmol. Astropart. Phys. **4**, 14 (2008).
[8] M. Viel, E. Branchini, K. Dolag, M. Grossi, S. Matarrese and L. Moscardini, Mon. Not. R. Astron. Soc. **393**, 774 (2009).
[9] C. Park *et al.*, Astrophys. J. **633**, 11 (2005).
[10] M. Grossi, E. Branchini, K. Dolag, S. Matarrese and L. Moscardini, Mon. Not. R. Astron. Soc. **390**, 438 (2008).
[11] A. Slosar, C. Hirata, U. Seljak, S. Ho and N. Padmanabhan, J. Cosmol. Astropart. Phys. **8**, 31 (2008).
[12] A. P. S. Yadav and B. Wandelt, Phys. Rev. Lett. **100**, 181301 (2008).
[13] A. Curto, E. Martínez-González, P. Mukherjee, R. B. Barreiro, F. K. Hansen, M. Liguori and S. Matarrese, Mon. Not. R. Astron. Soc. **393**, 615 (2009).
[14] P. Vielva and J. L. Sanz, Mon. Not. R. Astron. Soc. **397**, 837 (2009).
[15] L.-Y Chiang, P. D. Naselsky and P. Coles, Astrophys. J. **664**, 8 (2007).
[16] C. Räth, G. E. Morfill, G. Rossmanith, A. J. Banday and K. M. Górski, Phys. Rev. Lett. **102**, 131301 (2009).
[17] D. Pietrobon, P. Cabella, A. Balbi, G. de Gasperis and N. Vittorio, Mon. Not. R. Astron. Soc. **396**, 1682 (2009).
[18] G. Rossi, R. K. Sheth, C. Park and C. Hernández-Monteagudo, Mon. Not. R. Astron. Soc. **399**, 304 (2009).
[19] M. Liguori, S. Matarrese and L. Moscardini, Astrophys. J. **597**, 57 (2003).
[20] P. Chingangbam and C. Park, J. Cosmol. Astropart. Phys. **12**, 19 (2009).
[21] U. Seljak and M. Zaldarriaga, Astrophys. J. **469**, 437 (1996).